

# Electrochemical Biochip for Applications to Wireless and Batteryless Monitoring of Free-Moving Mice

Camilla Baj-Rossi, Giovanni De Micheli and Sandro Carrara\*

**Abstract**—A multi-sensing platform for applications in wireless and batteryless monitoring of free-moving small animals is presented in this paper. The proposed platform hosts six sensors: four biosensors for sensing of both disease biomarkers and therapeutic compounds, and two further sensors (T and pH) for biosensor calibration. Electrodeposition of *Multi-Walled Carbon Nanotubes* (MWCNTs) and the subsequent functionalization with proper enzymes is used to assure sensitivity and specificity in electrochemical biosensing. The realized sensors are demonstrated to be capable of measuring several parameters: lactate with a sensitivity of  $77 \pm 26 \mu\text{A}/\text{mM} \cdot \text{cm}^2$  and a limit of detection (LOD) of  $4 \pm 1 \mu\text{M}$ ; glucose with a sensitivity of  $63 \pm 15 \mu\text{A}/\text{mM} \cdot \text{cm}^2$  and a LOD of  $8 \pm 2 \mu\text{M}$ ; Etoposide (a well known anti-cancer agent) with a sensitivity of  $0.15 \pm 0.04 \text{ mA}/\text{mM} \cdot \text{cm}^2$  and a LOD of  $4 \pm 1 \mu\text{M}$ ; Open Circuit Potential (OCP) measurements are used on a Pt/IrOx junction to sense pH with a sensitivity of around  $-75 \pm 5 \text{ mV}/\text{pH}$ ; while a Pt resistive thermal device is used to measure physiological temperature-range with an average sensitivity of  $0.108 \pm 0.001 \text{ k}\Omega/^\circ\text{C}$ .

## I. INTRODUCTION

Translational medicine makes a quite large use of mice especially as good and low-cost models of mammalian regulators function by monitoring, *e.g.*, the ATP [1]. Monitoring free-moving animal is an extremely good approach because translational medicine may monitor the disease evolution in a more natural dynamics by following the animal models in a situation with reduced stress. Of course, batteries are not allowed on board due to size constrains when dealing with very small animals. Batteryless passive systems are easily possible in animal monitoring because the implant does not require any on-board power consumption [2]. On the other hand, the use of cameras mounted on the mouse cage provides low-cost solutions for continuous monitoring of the behavior of free-moving mice [3]. However, active devices are definitely required if we want to integrate biosensors on the implant and, therefore, systems for wireless power delivery in mouse telemetry have been proposed few years ago [4]. This new advance opened the possibility to develop active systems for continuous monitoring of free-moving mice even dealing with metabolites detection. New systems have been then proposed for monitoring of free-moving mice dealing with blood pressure [5], body temperature and heart pulse [6]; while remotely powered detection of pH was demonstrated too [7]. Also the possibility of multi-channel devices has

been demonstrated though only limited to applications in ECG acquisitions [8]. These very recent developments show detection of bio-signals but not metabolites. For molecular metabolites the story is quite different because it is typically needed to involve enzymes-based biosensors that require more complex integration of bio-membranes and electronics. In the area of metabolism monitoring in small animals, the most successful development is the monitoring of glucose in mice [9], even with implants remaining *in-vivo* up to 56 days [10]. More recent devices have shown detection of other endogenous metabolites (*e.g.*, lactate, glutamate, and ATP) [11] though not within the same sensing platform. However, all these more recent developments still present electrical cables through the animals' skin [9]–[12], which allow only limited movement in the animal cage. In 2012, a novel system to transmit power and receive data on completely free-moving animals has been proposed [13], and at the end of last year the possibility of the integration with a fully implantable and biocompatible multi-panel array sensor has been proposed [14]. Aim of the present paper is to present the most recent outputs toward the development of this novel multi-array sensor platform and to demonstrate the feasibility to detect several endogenous metabolites (*e.g.*, glucose, lactate) and drugs (*e.g.*, *etoposide* (ETO), *mitoxantrone* (MTX), and *etodolac* (ETD) together with the sensing of pH and temperature for biosensors calibration. The biosensors were, in some cases, then functionalized with specific enzymes to assure specificity and MWCNT to assure high sensitivity for lactate and glucose [15] as well as for drugs [16]. This passive platform is tested here with laboratory equipment meanwhile it is built to be coupled with an active and fully implantable potentiostat [17] and with a wireless powering system for power and data transmission, for further applications in implantable devices for monitoring of free-moving mice in a cage.

## II. MATERIALS AND METHODS

### A. Application scenario

The fully-implantable device consists of three main building blocks: 1) a passive sensing platform, 2) integrated circuits (ICs) to perform electrochemical measurements and 3) a coil for power supply and data transmission. Fig. 1 shows a photograph of the implantable device after the assembly of the different components. The device in Fig. 1 is a not-working prototype that was intended to test the biocompatibility of the materials used [14]. This work will present a complete *in-vitro* characterization of the passive platform, while the electronics measurements for data communication

\*Corresponding author: [sandro.carrara@epfl.ch](mailto:sandro.carrara@epfl.ch)  
Laboratory of Integrated Systems, Swiss Federal Institute of Technology (EPFL), Lausanne, Switzerland  
The SNF Sinergia Project (CRSII2\_147694/1) and NanoSys project within the frame of the UE program ERC-2009-AdG-246810, financially supported this research.

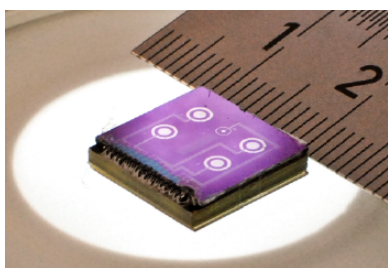


Fig. 1. Photograph of the implantable chip after the assembly of the components.

and remote powering are reported in another article [18].

### B. Passive Chip Microfabrication

Microfabrication was realized at the EPFL Centre of Micronano Technology (CMI). Silicon wafers with 500 nm of native oxide were chosen as substrate. Chip metalization was realized by evaporation of 10 nm of Ti, followed by 100 nm of Pt. Metal passivation was made via atomic layer deposition of  $Al_2O_3$ , followed by dry etching with Argon Ion Milling. More details on the microfabrication can be found in [14].

### C. Materials

MWCNTs ( $\sim 10$  nm diameter and  $\sim 1$ - $2$   $\mu m$  length) with 5%  $-COOH$  groups content, were purchased as a powder from DropSens (Spain). MWCNTs in powder were dispersed in a chitosan solution (0.7% w/v) pH 5 and then sonicated for 3 h to obtain a 8 mg/ml dispersion. All experiments were carried out in a 100 mM phosphate buffered saline solution (PBS, pH 7.4) as supporting electrolyte. Lactate oxidase (LOx) from *Pediococcus species* and glucose oxidase (GOx) from *Aspergillus Niger* were purchased from Roche in lyophilizate powder and dissolved in a 100 mM PBS (pH 7.4). Lithium L-lactate and D-(+)-glucose (Sigma-Aldrich, Switzerland) in powder and dissolved in in PBS. The drugs ETO, MTX and ETD purchased as a powder (Sigma-Aldrich) were dissolved in Dimethyl sulfoxide due to their low solubility in water. For the pH sensor, a solution of Iridium(IV) chloride hydrate (99.9% metals basis, from Sigma Aldrich),  $H_2O_2$  (30%), oxalic acid dihydrate (98%, from Sigma Aldrich), and potassium carbonate anhydrous (99%, from Alfa Aesar) was prepared for the deposition of the Iridium Oxide film (IrOx), as described in [19].

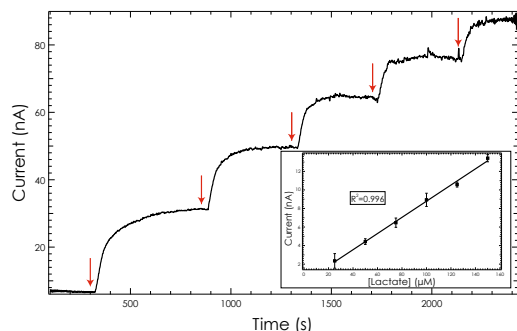


Fig. 2. Calibration line of lactate detection in CA (at a fix potential of +650 mV) after functionalization with MWCNTs and LOx. Error bars correspond to the standard deviation for 3 different measurements (confidence interval 95.4%).

### D. Electrode preparation and functionalization

For the detection of lactate and glucose in *chronoamperometry* (CA), working electrodes were functionalized by electrodeposition of a chitosan/MWCNT dispersion 8 mg/ml as described in [14]. For glucose and lactate measurements, we used *working electrodes* (WEs) with a diameter of 500  $\mu m$  and 1.2 mm, respectively. A 33 mg/ml solution of LOx, or, alternatively, a 15 mg/ml solution of GOx, was drop cast on some working electrodes and stored overnight at 4°C. For the measurements in the presence of drugs with *cyclic voltammetry* (CV), the electrodes were used without modifications. For the pH sensor, we used a working electrode of 300  $\mu m$  diameter. A layer of IrOx was created on the electrode surface by applying a constant current of 0.94  $\mu A$  for 500 s. After 2 days of stabilization in PBS pH 7.4 to reduce the potential drift, the electrodes were tested for pH sensing. All the samples were freshly prepared and used the same day. When not in use, electrodes were stored at 4°C.

### E. Electrochemical Measurements

To test the passive sensing platform, electrochemical measurements were performed using an Autolab electrochemical workstation (Metrohm, Switzerland). Electrodes were tested for lactate and glucose sensitivity with CA at +650 mV. The sensors were first dipped in a 100 mM PBS solution (pH 7.4), under stirring conditions, then conditioned for 1 h at +650 mV and then tested against repeated injections of lactate 25  $\mu M$ , or glucose 50  $\mu M$ . CV was used to identify the oxidation/reduction peaks of ETO, MTX and ETD. CV was performed at room temperature under aerobic conditions by applying a triangular waveform voltage in the range between -700 mV and +700 mV vs. Pt and a scan rate of 20 mV/s. After an initial conditioning in PBS, which consists of 30' of continuous cycling, drops of 400  $\mu l$  of ETO or MTX solutions were added at the right concentration. pH was computed averaging the *open circuit potential* (OCP) by continuously changing the pH of the buffer solution by adding an acid or a basic solution (HCl and NaOH, respectively). The pH was monitored by means of an external pH meter (from VWR). An external reference electrode (double junction in Ag|AgCl) was used in

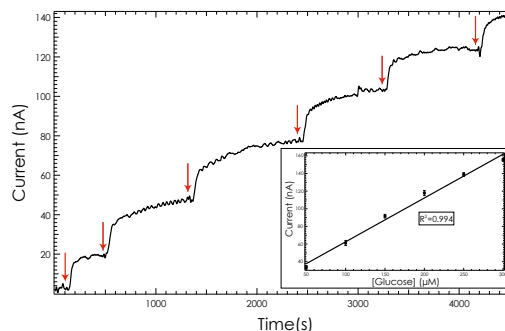


Fig. 3. Calibration line of glucose detection in CA (at a fix potential of +650 mV) after functionalization with MWCNTs and GOx. Error bars correspond to the standard deviation for 3 different measurements (confidence interval 95.4%).

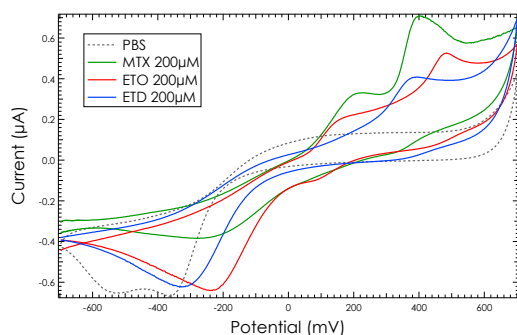


Fig. 4. Cyclic voltammograms of a bare electrode in PBS, in the presence of MTX 200 $\mu$ M, ETO 200 $\mu$ M or ETD 200 $\mu$ M.

order to have stable and reproducible measurements. For the temperature sensor, a Fluke 87V Industrial multimeter (by Fluke) was connected to our platform to measure the changes in resistivity. Sensitivity and *limit of detection* (LOD) are the key parameter used to evaluate the sensing performances. Sensitivity per unit area was computed from the slope of the straight line obtained by plotting the current increases *vs.* glucose, lactate or drug concentration. The LOD was computed as three times the signal-to-noise ratio according to the expression  $LOD = k \frac{\delta i}{S}$ , where  $\delta i$  is the standard deviation of the blank measurements,  $S$  is the sensitivity, and  $k$  is a parameter accounting for the confidence level ( $k = 1, 2, \text{ or } 3$  corresponds to 68.2%, 95.4%, or 99.6% of statistical confidence) [20].

### III. RESULTS AND DISCUSSION

#### A. Measurements of metabolites and anti-cancer drugs

After the electrodeposition of MWCNTs in chitosan and the functionalization of the WE with the enzyme, electrodes were tested for lactate and for glucose sensitivity with CA at +650 mV. The CA measurements at +650 mV for lactate and glucose are reported in Fig. 2 and Fig. 3, respectively. The arrows correspond to repeated injections of lactate 25 $\mu$ M or glucose 50  $\mu$ M, respectively. Well-defined current steps are visible every further injection. The calibration lines reported in the insets of Fig. 2 and Fig. 3 are calculated from the evaluation of the current steps, by measuring the difference between the reached current value and the baseline. For lactate we obtained a sensitivity of  $77 \pm 26 \mu\text{A}/\text{mM} \cdot \text{cm}^2$  and a LOD of  $4 \pm 1 \mu\text{M}$ , while for glucose we obtained a sensitivity of  $63 \pm 15 \mu\text{A}/\text{mM} \cdot \text{cm}^2$  and a LOD of  $8 \pm 2 \mu\text{M}$ , which fits with many clinical applications [21]. Calibration of glucose and lactate at higher physiological concentrations will require the adoption of a system of membranes, as reported in [22], and it will be the object of our future investigations. However, with our sensing platform, we can monitor many other metabolites of clinical interest (*e.g.* glutamate, ATP), by changing the enzyme.

The anti-cancer drugs ETO and MTX, and the anti-inflammatory drug ETD were monitored with CV. CV has been widely used to detect electroactive drugs in biological fluids [23]. As reported in previous studies [24]–[26], ETO, MTX and ETD are electro-active compounds that give in CV well-defined oxidation peaks in the potential window

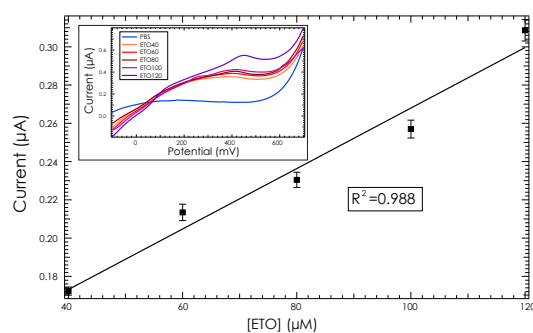


Fig. 5. Calibration curve for ETO within the physiological range in PBS, obtained in CV. Error bars correspond to the standard deviation for 4 different measurements (confidence interval 95.4%). The inset shows the oxidation peak currents increasing with the drug concentration.

between +100 mV and +700 mV. Fig. 4 shows the cyclic voltammograms for a bare electrode (500  $\mu\text{m}$  diameter) in PBS or in the presence of 200  $\mu\text{M}$  MTX, or 200  $\mu\text{M}$  ETO or 200  $\mu\text{M}$  ETD. According to literature, the voltammograms show two defined oxidation peaks for ETO (at +200 mV and +500 mV *vs.* Pt), two oxidation peaks for MTX (at +250 mV and +450 mV *vs.* Pt), and an oxidation peak for ETD (at +350 mV *vs.* Pt). With bare electrodes, we also performed CV measurements to calibrate the sensors for ETO within the therapeutic range. Fig. 5 shows the dependence of the peak current on ETO concentrations. The y-axis values are the peak values of the current peaks centered at +500 mV. The inset in Fig. 5 shows the linear increase in current of the oxidation peaks at various ETO concentrations, with a sensitivity of  $0.15 \pm 0.04 \text{ mA}/\text{mM} \cdot \text{cm}^2$  and a LOD of  $4 \pm 1 \mu\text{M}$ , which fits ETO therapeutic range (33.9–101.9, [27]). These results prove that the sensing platform is capable to monitor drugs and metabolites within their therapeutic or physiological ranges.

#### B. Temperature sensor

The temperature sensor is a *resistive thermal device* (RTD) that consists of a Pt wire of 4  $\mu\text{m}$  width and 93 mm length, with an average resistivity of 34  $k\Omega$  at 20 $^\circ\text{C}$ . We chose Pt since it is commonly used for resistive thermal devices and because, among other metals Pt represents the best trade-off between linear behavior, higher metal resistivity and biocompatibility [28]. Fig. 6 shows the response of the Pt-RTD upon different temperatures in PBS. The temperature was first increased from 35 $^\circ\text{C}$  to 42 $^\circ\text{C}$  (forward scan) and then was inversely changed (backward scan), showing a linear behavior with an average sensitivity of  $0.108 \pm 0.001 k\Omega/^\circ\text{C}$ , which is compatible with the theoretical value of 0.13  $k\Omega/^\circ\text{C}$  (calculated from the temperature coefficient of resistivity for Pt,  $\alpha = 0.00385^\circ\text{C}^{-1}$ ).

#### C. pH sensor

IrOx is a well-known biocompatible material already used in the creation of implantable electrodes [19]. The OCP of an IrOx film changes in a predictable manner according to the pH of the solution. Fig. 7 shows the calibration of the pH sensor measured in the pH range from 5 to 9. The pH of the buffer solution was continuously monitored with an

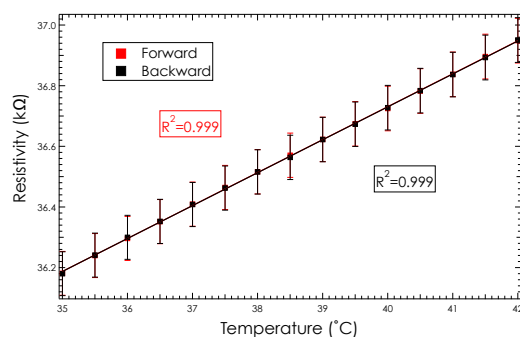


Fig. 6. Calibration curve for the temperature sensor. Error bars correspond to the standard deviation for 9 different measurements (confidence interval 95.4%).

external pH meter and the corresponding OCP was measured for the forward scan (pH from 5 to 9) and for the backward scan (pH from 9 to 5). In the considered range, the potential changes linearly with increasing pH, with a sensitivity of  $-74 \pm 3$  mV/pH for the forward scan, and  $-75 \pm 5$  mV/pH for the backward scan. Our sensor with the IrOx film showed a near super-Nernstian response with sensitivity values similar to the ones reported in [19].

#### IV. CONCLUSIONS

Aim of the present paper was to present the most advanced developments of a novel multi-array sensor platform for further applications in monitoring of free-moving mice. The paper demonstrated the feasibility of the multi-panel platform for acquiring data among several endogenous metabolites related to animal metabolism as well as several exogenous compounds, typically therapeutic drugs. The platform also demonstrated the reliability of the acquired data by hosting sensors for data calibration. The detection of glucose, lactate, ETO, MTX, and ETD is shown as proof of the platform capability for metabolism monitoring, while the detection of pH and temperature is shown as proof of biosensors calibration. The passive sensing platform presented in this work is built to be integrated into a fully-implantable device for further applications in monitoring of mice that are free to move in a cage. In particular, the device will be used to monitor concentrations of drugs and disease biomarkers in interstitial tissues of very small animals.

#### ACKNOWLEDGMENT

Sara S. Ghoreishizadeh, Enver G. Kilinc, Catherine Dehollain, Tanja Rezzonico Jost and Fabio Grassi are acknowledged for useful discussions on the design of the passive platform.

#### REFERENCES

- [1] U. Schenk, M. Frascoli, M. Proietti, R. Geffers, E. Traggiai, J. Buer, C. Ricordi, A. M. Westendorf, and F. Grassi, *Science signaling*, vol. 4, no. 162, p. ra12, 2011.
- [2] T. Kaya and H. Koser, in *IEEE RFID Eurasia, 1st Annual*, 2007, pp. 1–4.
- [3] G. Stamatescu, K. Romer, R. Ludwig, S. M. Ibrahim, and V. Sgârciu, in *IEEE DCOSS, 2011*, pp. 1–3.
- [4] D. Russell, D. McCormick, A. Taberner, P. Nielsen, P. Hu, D. Budgett, M. Lim, and S. Malpas, in *IEEE BioCAS 2009*, pp. 273–276.
- [5] P. Cong, N. Chaimanonart, W. H. Ko, and D. J. Young, *Solid-State Circuits, IEEE J.*, vol. 44, no. 12, pp. 3631–3644, 2009.

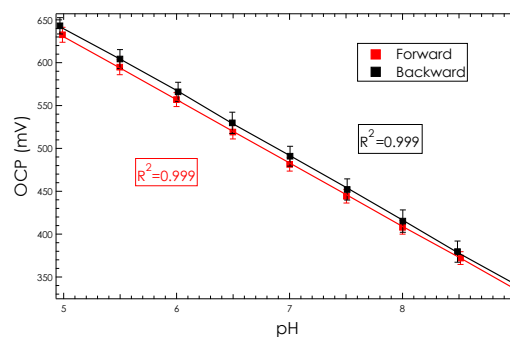


Fig. 7. Open circuit potential of the IrOx coated electrode to different pH. Error bars correspond to the standard deviation for 9 different measurements (confidence interval 95.4%).

- [6] N. Chaimanonart and D. J. Young, in *IEEE EMBC 2009*, pp. 4872–4875.
- [7] H. Cao, V. Landge, U. Tata, Y.-S. Seo, S. Rao, S.-J. Tang, H. Tibbals, S. Spechler, and J. Chiao, *Biomed. Engin., IEEE Trans.*, vol. 59, no. 11, pp. 3131–3139, 2012.
- [8] C.-C. Liu, E. O'Connor, and K. P. Strohl, *Sensors Journal, IEEE*, vol. 6, no. 1, pp. 187–202, 2006.
- [9] U. Klueh, Z. Liu, B. Cho, T. Ouyang, B. Feldman, T. P. Henning, M. Kaur, and D. Kreuzer, *Diabet. techn. & ther.*, vol. 8, no. 3, pp. 402–412, 2006.
- [10] B. Yu, N. Long, Y. Moussy, and F. Moussy, *Biosens. Bioelectr.*, vol. 21, no. 12, pp. 2275–2282, 2006.
- [11] S. Carrara, L. Bolomey, C. Boero, A. Cavallini, E. Meurville, G. De Micheli, T. R. Jost, M. Proietti, and F. Grassi, *Sensors Journal, IEEE*, vol. 13, no. 3, pp. 1018–1024, 2013.
- [12] U. Klueh, Z. Liu, B. Feldman, T. P. Henning, B. Cho, T. Ouyang, and D. Kreuzer, *J. Diabetes Sci. Technol.*, vol. 5, no. 3, pp. 583–595, 2011.
- [13] E. G. Kilinc, F. Maloberti, and C. Dehollain, in *IEEE BioCAS 2012*, pp. 260–263.
- [14] C. Baj-Rossi, E. G. Kilinc, S. S. Ghoreishizadeh, D. Casarino, T. R. Jost, C. Dehollain, F. Grassi, L. Pastorino, G. De Micheli, and S. Carrara, in *IEEE BioCAS 2013*, pp. 166–169.
- [15] C. Boero, S. Carrara, G. Del Vecchio, L. Calzà, and G. De Micheli, *NanoBioscience, IEEE Trans.*, vol. 10, no. 1, pp. 59–67, 2011.
- [16] S. Carrara, A. Cavallini, V. Erokhin, and G. De Micheli, *Biosens. Bioelectr.*, vol. 26, no. 9, pp. 3914–3919, 5 2011.
- [17] S. Ghoreishizadeh, E. G. Kilinc, C. Baj-Rossi, G. De Micheli, C. Dehollain, and S. Carrara, in *IEEE BioCAS 2013*, pp. 218–221.
- [18] C. Baj-Rossi, E. G. Kilinc, S. S. Ghoreishizadeh, D. Casarino, J. T. Rezzonico, C. Dehollain, F. Grassi, L. Pastorino, G. De Micheli, and S. Carrara, *IEEE Transaction on Biomedical Circuits and Systems*, 2014, Submitted.
- [19] I. A. Ges, B. L. Ivanov, D. K. Schaffer, E. A. Lima, A. A. Werdich, and F. J. Baudenbacher, *Biosens. Bioelectr.*, vol. 21, no. 2, pp. 248–256, 2005.
- [20] J. Mocak, A. Bond, S. Mitchell, and G. Scollary, *Pure Appl. Chem.*, vol. 69, no. 2, pp. 297–328, 1997.
- [21] V. H. Routh, *Physiol. behav.*, vol. 76, no. 3, pp. 403–413, 2002.
- [22] S. P. Nichols, A. Koh, W. L. Storm, J. H. Shin, and M. H. Schoenfish, *Chemical reviews*, vol. 113, no. 4, pp. 2528–2549, 2013.
- [23] N. Abo El-Maali, *Bioelectrochem.*, vol. 64, no. 1, pp. 99–107, 2004.
- [24] J. Holthuis, W. Van Oort, F. Römken, J. Renema, and P. Zuman, *J. Electroanal. Chem. Interf. Electrochem.*, vol. 184, no. 2, pp. 317–329, 1985.
- [25] A. Oliveira Brett, T. Macedo, D. Raimundo, M. Marques, and S. Ser-rano, *Anal. chim. acta*, vol. 385, no. 1, pp. 401–408, 1999.
- [26] S. Yilmaz, B. Uslu, and S. A. Özkan, *Talanta*, vol. 54, no. 2, pp. 351–360, 2001.
- [27] J. J. Holthuis, P. E. Postmus, W. J. Van Oort, B. Hulshoff, H. Verleun, D. T. Sleijfer, and N. H. Mulder, *Europ. J. Canc. Clin. Onc.*, vol. 22, no. 10, pp. 1149–1155, 1986.
- [28] R. I. Frank and T. E. Salzer, U.S. Patent No. 4,129,848., 12 1978.